THE ASTROPHYSICAL JOURNAL, 386:720–728, 1992 February 20

THE EFFECT OF ELECTRON COLLISIONS ON ROTATIONAL POPULATIONS OF COMETARY WATER

XINGFA XIE[1] AND MICHAEL J. MUMMA[2]
Laboratory for Extraterrestrial Physics, Code 693, NASA/Goddard Space Flight Center, Greenbelt, MD 20771
Received 1991 May 13; accepted 1991 August 22

ABSTRACT

The e–H_2O collisional rate for exciting rotational transitions in cometary water is evaluated for conditions found in comet Halley during the *Giotto* spacecraft encounter. In the case of the $0_{00} \rightarrow 1_{11}$ rotational transition, the e–H_2O collisional rate exceeds that for excitation by neutral-neutral collisions at distances exceeding 3000 km from the cometary nucleus. The estimates are based on theoretical and experimental studies of e–H_2O collisions, on ion and electron parameters acquired in situ by instruments on the *Giotto* and *Vega* spacecraft, and on results obtained from models of the cometary ionosphere. Thus, the rotational temperature of the water molecule in the intermediate coma may be controlled by collisions with electrons rather than with neutral molecules, and the rotational temperature retrieved from high-resolution infrared spectra of water in comet Halley may reflect electron temperatures rather than neutral gas temperatures in the intermediate coma. The contribution of electron collisions may explain the need for large H_2O–H_2O cross sections in models which neglect the effect of electrons. The importance of electron collisions is enhanced for populations of water molecules in regions where their rotational lines are optically thick.

Subject headings: atomic processes — comets: individual (Halley) — molecular processes

1. INTRODUCTION

Investigations of comet Halley during encounters of the *Giotto* and *Vega* spacecraft and through observations with space-based (*IUE*), airborne (Kuiper Airborne Observatory and Lear Jet Observatory), and ground-based telescopes, resulted in major advances in our understanding of its chemical composition and of the physical conditions and processes in the cometary coma. While in situ measurements provided direct information on conditions in the intermediate coma during the spacecraft encounters, it is the Earth-based spectroscopy of parent molecules, especially water vapor (the dominant volatile species in the comet), that offers a remote but direct probe of physical conditions there. However, these conditions may be retrieved from spectral data only if the processes that control rotational populations and spectral line formation are well understood. From the studies of Weaver & Mumma (1984), Crovisier (1984), and Bockelee-Morvan (1987), it was accepted that water rotational populations are determined by fluorescence of direct solar radiation in the outer coma and by neutral particle collisions in the inner coma, with the cross-over point depending on the neutral gas density.

Two recent theoretical studies achieved satisfactory fits to the line-by-line intensities revealed in infrared spectra of the ν_3 band of water in comet Halley acquired on the Kuiper Airborne Observatory (KAO) (Mumma et al. 1986; Weaver, Mumma, & Larson 1987; Larson et al. 1989). In the first, Bockelee-Morvan (1987) applied the escape probability formalism to treat optical trapping of the water rotational lines and to synthesize individual lines of the ν_2 and ν_3 bands. She obtained satisfactory fits to the pre- and post-perihelion spectra of comet Halley by using a H_2O–H_2O cross section of 5×10^{-14} cm^2 for rotational transitions. However, the use of such a large cross section is questionable, as is the validity of the escape probability method for the cometary atmosphere. More recently, Storrs & Mumma (1991) included multiple scattering and studied the effect of optical depth by explicit numerical integration of the equation of radiation transfer. They applied their model to the KAO pre-perihelion observations of comet Halley and found that the best fits required very large H_2O–H_2O cross sections ($\sim 10^{-12}$–10^{-11} cm^2) for rotational transitions. They suggested the need for such a large cross section could indicate that other processes, such as electron or ion collisions, were affecting rotational excitations. The role of electron collisions was examined briefly by Bockelee-Morvan (1987). She adopted an electron temperature of 5×10^4 K and an electron density of 2×10^3 cm^{-3} at 1000 km from the nucleus, and estimated the excitation rate from electrons to be about 8×10^{-4} s^{-1}, i.e., much smaller than the water-water collisional rates ($\sim 4 \times 10^{-2}$ s^{-1}). She therefore neglected electron collisions in her model. However, measurements from *Giotto* and *Vega* (Ip & Axford 1990; Pedersen et al. 1987) revealed an electron density of 10^4 cm^{-3} at 1000 km distance, and theoretical study of the cometary ionosphere (Körömezey et al. 1987) indicated that the electron temperature followed that of the neutral gas (60–100 K) inside the contact surface ($r = 4500$ km). The combination of higher density and lower temperature (larger cross section) could make electron collisions nonnegligible in exciting water rotational transitions.

In this paper, we examine the role of electron and ion collisions in controlling H_2O rotational populations in comet Halley. We first review the theoretical and experimental results for e–H_2O and H_2O–H_2O cross sections, and the physical conditions of electrons in the coma. Next, we discuss physical processes affecting rotational populations in cometary water and estimate collision rates for H_2O–H_2O and e–H_2O interactions, and we examine the importance of electron collisions in the intermediate coma. We demonstrate that electron-water collisions play an important role in populating rotational energy levels of water molecules in the coma, even if the largest

[1] Also Astronomy Department, University of Pennsylvania, Philadelphia, PA 19104.
[2] Chief Scientist, Planetary and Astrophysical Sciences.

possible H_2O–H_2O cross section (5×10^{-14} cm^2) is used. However, we show that the effective H_2O–H_2O cross section is probably far smaller, making e–H_2O collisions even more important over much of the coma. We give a brief discussion of the impact of optical trapping on rotational populations, and of the effect of electron collisions in comets with different gas production rates. Finally, we examine the role of ion-molecule collisions; however, quantitative calculation is hindered by the lack of cross sections for energies below 0.1 eV.

2. COLLISIONAL CROSS SECTIONS FOR WATER ROTATIONAL TRANSITIONS

2.1. e–H_2O *Collisional Cross Sections*

Theoretical calculations have shown that the cross sections for rotational transitions are very large for molecules such as H_2O, with large permanent dipole moments (Itikawa 1972; Dickinson & Richards 1975; Jain & Thompson 1983). Itikawa (1972) used the Born approximation to calculate the cross section for rotational transitions by e–H_2O collisions, which cross section is formulated as follows:

$$\sigma_{J K_a K_c \to J' K'_a K'_c} = \frac{8\pi}{3k^2}(2J' + 1)D^2 \times \langle J'_{K'_a K'_c} | J_{K_a K_c} \rangle^2 \ln\frac{k + k'}{k - k'}, \quad (1)$$

where $D = 1.85$ debye is the permanent dipole moment of the water molecule; J, K_a, and K_c are quantum numbers for the initial state of the transition and J', K'_a, and K'_c for the final state; and k and k' are the initial and final wave numbers of the electron. The factor $\langle J'_{K'_a K'_c} | J_{K'_a K'_c} \rangle$ is closely related to the line strength in the following form (King, Hainer, & Cross 1947; Schwendeman & Laurie 1958):

$$S = (2J' + 1)(2J + 1)\langle J'_{K'_a K'_c} | J_{K_a K_c} \rangle^2 . \quad (2)$$

In addition, Itikawa (1972) has shown theoretically that dipole-induced rotational transitions are much more effective (by approximately two orders of magnitude) than any multipole interactions. The more elaborate theoretical calculations of Jain & Thompson (1983) confirmed that the Born approximation is very good for H_2O rotational transitions at electron impact energies of 2.14 eV and 6.0 eV. We will use Itikawa's formula in our estimates. At the collisional energy of 0.01 eV the cross section calculated from equation (1) for the $0_{00} \to 1_{11}$ rotational transition is about 3×10^{-13} cm^2 at the peak. Figure 1*b* shows the cross sections calculated from equation (1) for a few transitions. Note that the peak cross section occurs at an electron energy $\sim 2\Delta E$, where ΔE is the energy difference for the transition in question. This will become important when we consider the mean electron energy in the cometary coma.

Sokolov & Sokolova (1982) reported total cross section measurements from their electron scattering experiments at low impact energy (Table 1). Christophorou & Pittman (1970) also reported a mean momentum transfer cross section of 3.04×10^{-13} cm^2 for e–H_2O interactions in a swarm measurement at the temperature 298 K ($E = 0.026$ eV). Measurements at two impact energies $E = 2.14$ eV and $E = 6.0$ eV (Jung et al. 1982) showed that the (inelastic) cross sections for rotational transitions are much larger than those for elastic scattering, and we also expect this to be so for electron impact at lower energies (at least for electron energies well above threshold).

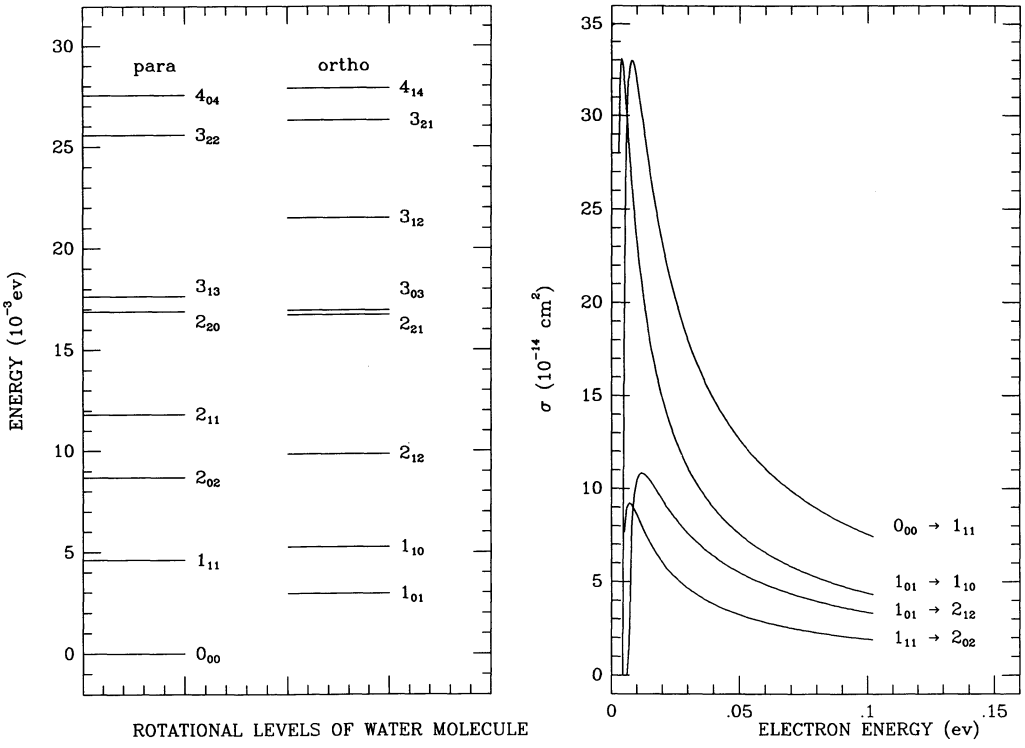

FIG. 1.—(*a*) The lower rotational levels of water in the ground vibrational state. (*b*) The electron-water collision cross sections for the lower four rotational transitions as a function of the impact energy (adapted from Itikawa 1972).

TABLE 1

TOTAL CROSS SECTION FOR ELECTRON-WATER SCATTERING[a]

E (eV)	σ_T (10^{-14} cm^2)	E (eV)	σ_T (10^{-14} cm^2)
0.01.....	30	1.0	0.6
0.02.....	20	2.0	0.3
0.04.....	15	3.0	0.2
0.06.....	11	4.0	0.14
0.08.....	8.0	5.0	0.12
0.10.....	6.0	6.0	0.11
0.50.....	1.5	7.0	0.10

[a] From Sokolov & Sokolova 1982.

Thus the total cross sections are dominated by inelastic processes, i.e., at low energies, by rotational excitation. For our purposes the results shown in Figure 1*b* are in acceptable agreement with those of Table 1.

These studies show that the theoretical and experimental results are quite consistent with each other, and that the rotational cross section for e–H_2O collisions is very large, of the order of 10^{-13} cm^2 at impact energy 0.02 eV.

2.2. H_2O–H_2O *Collisional Cross Sections*

The H_2O–H_2O cross section is usually taken to be 5×10^{-14} cm^2 in the literature. This estimate is based on measurements by Bauer, Godon, & Duterag (1985) of collisional broadening of the $2_{20} \rightarrow 3_{13}$ 183 GHz line of water at $T = 251$–299 K and by Murphy & Boggs (1969) of several additional rotational lines at 300 K. In all cases, kT (~ 200 cm^{-1}) is much larger than the corresponding transitional energy ΔE (e.g., $\Delta E \sim 5.5$ cm^{-1} for the 183 GHz line). However, the cross section derived from the collision-broadened linewidth is the total cross section, i.e., the sum of the elastic and inelastic processes for upper and lower energy levels. The inelastic part is the sum of the de-excitational and excitational contribution from the upper energy level to other energy levels and from the lower energy level. Thus, the excitation cross section for the relevant transition may account for only a small portion of the total inelastic cross section (Van Regemorter 1965). Furthermore, for rotationally relaxed water ($T_{rot} \sim 60$ K in the comet), the typical transition energies are 20–50 cm^{-1}, while kT is only ~ 41 cm^{-1}. Thus many transitions (those with $\Delta E \geq kT$, e.g., $1_{01} \rightarrow 2_{12}$) cannot be excited by neutral-neutral collisions if $T \sim 60$ K, since the translational-rotational process is below threshold. For most cases (typically, $\Delta E \sim 50$ cm^{-1}) the process is so close to threshold that the excitation cross section for the transition is far less than the total cross section (2.6×10^{-14} cm^2 at 251 K) derived from the self-broadening of the 183 GHz line (Bauer et al. 1985). Therefore, the significance of neutral-neutral collisions has been greatly overestimated.

Because of the large e–H_2O cross section at low impact energies, it is possible that electron collisions may dominate over neutral collisions under certain conditions. We will continue to use the value of 5×10^{-14} cm^2 for an initial comparison of H_2O–H_2O collisional excitational rates, but we recognize that this will almost certainly overstate their significance.

3. THE COLLISIONAL ENVIRONMENT IN COMET HALLEY

3.1. *The Electron Density Profile in the Coma*

In the coma of comet Halley, measurements of ion densities and temperatures were obtained by instruments on the spacecraft *Giotto* and *Vega* (Balsiger et al. 1986; Lämmerzahl et al. 1987). In the inner coma, the total ion density falls as $1/r$ as the result of the equilibrium between ionization and electron recombination, while in the outer region, it falls approximately as $1/r^2$, indicating radial outflow of ions (Balsiger et al. 1986; Neugebauer 1990). Pedersen et al. (1987) reported the electron density to be $\sim 10^3$ cm^{-3} at 5×10^4 km from *Vega 1* measurements (1986 March 6). This exceeds the ion density measured by *Giotto* (1986 March 14) by a factor of ~ 4.5, but since Halley's comet exhibited significant short-term variability in its gas production rate, we have adopted the *Giotto* parameters for self-consistency. We assume charge neutrality, and take the electron density to be equal to the total ion density shown in Figure 2. The electron density (n_e) is parameterized as

$$\begin{cases} \dfrac{1.3 \times 10^7}{r}\ \text{cm}^{-3} & r < 7280\ \text{km} \\ 1.7 \times 10^{-2} r^{1.3}\ \text{cm}^{-3} & 7280\ \text{km} < r < 1.25 \times 10^4\ \text{km} \\ 5.6 \times 10^3 \left(\dfrac{10^4}{r}\right)^2\ \text{cm}^{-3} & 1.25 \times 10^4\ \text{km} < r < 2.0 \times 10^5\ \text{km}, \end{cases} \quad (3)$$

(after Ip & Axford 1990), where r is the cometocentric distance in km. The corresponding H_2O production rate at the *Giotto* encounter was about 5×10^{29} molecules s^{-1} (Krankowsky et al. 1986).

3.2. *The Electron Temperature Profile in the Coma*

Although *Giotto* was not equipped to detect cold electrons ($E < 10$ eV), in situ measurements from *Giotto* of the ion temperature (Lämmerzahl et al. 1987 and Schwenn et al. 1987) showed it to increase from 160 K (0.014 eV) near 1700 km to 250 K (0.022 eV) near the contact surface. At the contact

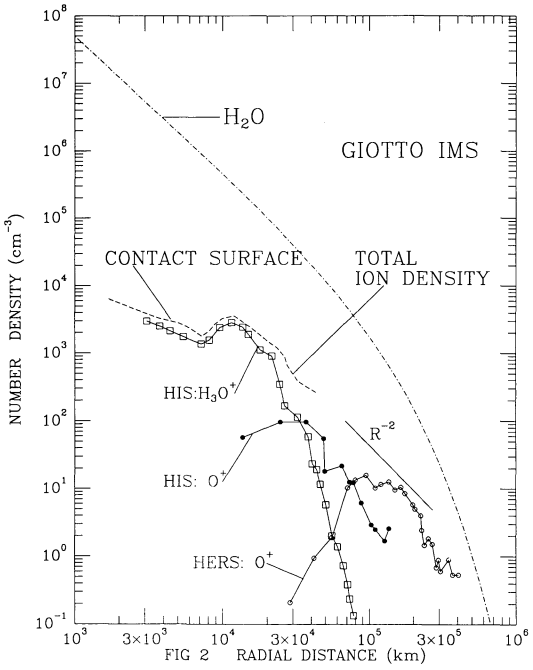

FIG. 2.—Cometocentric number densities for ions (after Ip & Axford 1990) and water for comet Halley at 0.9 AU. Water densities were obtained from the measured production rate of 5×10^{29} molecules s^{-1}, assuming uniform symmetric outflow (1 km s^{-1}).

surface the ion temperature rises by ~ 1000 K within less than 380 km and increases steadily farther out, reaching 5000 K (0.43 eV) at 1.5×10^4 km. Measurements of electrons in the outer coma were obtained from *Vega 1* and *Vega 2* as reported by Pedersen et al. (1987). They found the mean electron kinetic temperature to be $\sim 1.2 \times 10^4$ K (1 eV) at the distance 0.8–1.0×10^5 km. The electron temperature in the inner coma is not known from the spacecraft data, but it should not deviate much from the ion temperature in the interval from the contact surface to the outer region of interest for this study. Because of the large cross sections of ions and electrons for inelastic collisions with water and the high density of water in the inner region, the ions and electrons are expected to be strongly coupled to the neutral gas and thus to approach the same bulk velocity and kinetic temperatures as neutral gas inside the contact surface, within which the magnetic field strength is zero.

The theoretical model of Körömezey et al. (1987) indicated that the electron temperature is relatively low with $T_e < 300$ K inside the contact surface and is a little warmer than the neutral gas temperature near the contact surface. Gan & Cravens (1990) studied the electron temperature profile outside the contact surface, where electron heat conduction becomes important. They showed that electron temperature increases steadily with radial distances outside the contact surface, and a sharp transition boundary near a cometocentric distance of 1.5×10^4 km separates a region characterized by cold ($T < 10^4$ K), thermal electrons (inside) from one characterized by hot isothermal electrons (outside). This boundary is located just at the distance where the total ion density was found to be enhanced by a factor of 2–3 (Balsiger et al. 1987; Ip & Axford 1990; Fig. 2 of this paper), and this enhancement is explained in terms of a sharp increase in electron temperature (Ip et al. 1987; Gan & Cravens 1990), which results in a sharp reduction in the electron-ion recombination rate.

In our evaluation, the electron temperature in the cometary coma is taken to be approximately equal to the ion temperature measured from *Giotto* (Lämmerzahl et al. 1987), although the electron temperature may be less than the ion temperature within the contact surface

$$T_e = \begin{cases} 200 \text{ K} & r < 4500 \text{ km} \\ 2000 \text{ K} & 4500 \text{ km} < r < 7280 \text{ km} \\ 5000 \text{ K} & 7280 \text{ km} < r < 1.25 \times 10^4 \text{ km} \\ 10000 \text{ K} & 1.25 \times 10^4 \text{ km} < r < 2 \times 10^5 \text{ km} . \end{cases} \quad (4)$$

We regard this distribution to be conservative, since lower electron temperatures in the range $4500 < r < 1.25 \times 10^4$ km would lead to greatly enhanced collisional rates for rotation-changing collisions.

3.3. *The Neutral Gas Temperature in the Coma*

The neutral gas temperature in the collision-dominated coma has been calculated by the hydrodynamic model (Combi 1989; Combi & Smyth 1988; Bockelee-Morvan & Crovisier 1987b) and simulated by the Monte Carlo method (Hodges 1990). Combi & Smyth (1988) performed a Monte Carlo simulation to determine the heating rate from thermalization of suprathermal hydrogen atoms produced from water photodissociation. This heating rate was later applied to the hydrodynamic model for the collision-dominated coma (Combi 1989). Bockelee-Morvan & Crovisier (1987b) included optical trapping in estimating radiative cooling for water rotational transitions in a dust-free coma and showed that the neutral gas temperature is about 60–80 K at distances ranging from 10^3 km to 3×10^4 km, for the production rate of 1×10^{30} molecules s^{-1}. The neutral gas temperature should be lower for a less active comet. The neutral gas temperature in this region retrieved from the KAO infrared spectra of cometary water was ~ 60 K (Bockelee-Morvan & Crovisier 1987a; Weaver et al. 1987), consistent with model calculations. We therefore take the neutral gas temperature to be 60 K in the intermediate coma, for the gas production rate of 5×10^{29} molecules s^{-1}.

4. ROTATIONAL POPULATIONS OF COMETARY WATER

4.1. *Physical Processes Controlling Rotational Populations*

In models which neglect electron collisions, the population of rotational levels is dominated in the inner coma by neutral-neutral gas collisions, leading to a Boltzmann distribution with rotational temperature equal to the local kinetic temperature, and in the outer coma by fluorescence of solar radiation and spontaneous decay, resulting in fluorescence equilibrium (Weaver & Mumma 1984; Bockelee-Morvan 1987). In the transitional region, the level populations are influenced by both of the above processes and are calculated by solving equations of statistical equilibrium for the rotational energy levels (Chin & Weaver 1984; Bockelee-Morvan 1987). However, it will become clear later in this section that the effects of electron collisions must also be included in the models. At the very least, the fluorescence-equilibrium region will be pushed farther outward in the coma.

4.2. *Collisional Rates for the* $0_{00} \rightarrow 1_{11}$ *Rotational Transition*

The collisional excitation rate (s^{-1}) for a given water molecule is given by

$$\nu = n_e \sigma_{H_2O-e} \langle V_e \rangle \quad (5)$$

where $\langle V_e \rangle$, the average velocity of the electrons, is equal to $(8kT/\pi m_e)^{1/2}$. The cross section σ_{H_2O-e} is taken according to Itikawa's formula (eq. [1]). Using equations (3) and (4), the collisional excitation rate (s^{-1}) for the rotational transition $0_{00} \rightarrow 1_{11}$ is

$$\nu_{e-H_2O} = \begin{cases} \dfrac{29}{r} \text{ s}^{-1} & r < 4500 \text{ km} \\ \dfrac{18}{r} \text{ s}^{-1} & 4500 \text{ km} < r < 7280 \text{ km} \\ 1.7 \times 10^{-8} r^{1.3} \text{ s}^{-1} & 7280 \text{ km} < r < 1.25 \times 10^4 \text{ km} \\ 45 \times \left(\dfrac{10^2}{r}\right)^2 \text{ s}^{-1} & 1.25 \times 10^4 \text{ km} < r . \end{cases} \quad (6)$$

On the other hand, for uniform spherical outflow, the neutral gas density becomes

$$n_{H_2O} = \frac{Q}{4\pi V r^2} , \quad (7)$$

where V is the expansion velocity of the neutral gas, taken as 1.0 km s^{-1} in the region a few thousand kilometers away from the nucleus. The H_2O–neutral gas cross section is approximately equal to the H_2O–H_2O cross section, which is taken to be 5×10^{-14} cm^2 for the time being. With the relative velocity of water molecules taken as $(16kT/\pi m_{H_2O})^{1/2}$, where the typical water temperature is ~ 60 K at a dis ance of a few thousand

kilometers, the water-neutral gas collision frequency at cometocentric radius r is given by

$$\nu_{H_2O-H_2O} = \frac{7.5 \times 10^4}{r^2} \text{ s}^{-1} . \quad (8)$$

4.3. *Rotational Populations of the Water Molecule in Comet Halley*

The excitation rates are shown in Figures 3*a*–6*a*. It is clear that for the $0_{00} \rightarrow 1_{11}$ rotational transition (Fig. 3*a*) the e–H_2O collisional excitation rate will be equal to that of H_2O–H_2O collisions somewhere near ~ 3000 km and will exceed the latter at greater distances. In the region where the electron collisional rate is comparable to or larger than that of neutral gas collisions, electron collisions will affect the rotational population. Vibrational infrared fluorescence can also produce rotational excitation. The total fluorescence rate (Weaver & Mumma 1984; Bockelee-Morvan 1987) at 0.9 AU is shown in Figure 3*a* and may be regarded as a rough measure of the rotational pumping rate from this term. We assume one quantum of rotational excitation per event. Clearly, infrared resonance fluorescence dominates rotational pumping only in the outer coma. De-excitation rates for four lower rotational transitions are shown in Figures 3*b*–6*b*, where the rates for relaxation by e–H_2O and H_2O–H_2O collisions are compared with radiative relaxation in the optically thin case. We have taken collisional relaxation rates from cross sections given by equation (1) for the de-excitation process.

4.4. *Optical Trapping of Rotational Lines*

In the above we estimated the excitation and de-excitation rates in the optically thin coma. However, for the active comet with a gas production rate of 5×10^{29} molecules s^{-1}, the critical radius corresponding to optical depth $\tau_c = 1.0$ is $\sim 1 \times 10^5$ km for the $0_{00} \rightarrow 1_{11}$, $1_{01} \rightarrow 1_{10}$, and $1_{01} \rightarrow 2_{12}$ transitions (Bockelee-Morvan 1987). Inside the critical radius, these rotational lines are optically thick.

Optical trapping in the optically thick region results in an efficient reduction in the Einstein A-coefficient (Crovisier 1984; Bockelee-Morvan 1987; Storrs & Mumma 1991). In an optically thin coma, each time the water molecule is excited from the lower level i to the higher level j, it spends a mean lifetime $\tau = (\sum_i A_{ji})^{-1}$ (A_{ji} is the Einstein A-coefficient of the transition) before radiative decay returns it to a lower level. But in the optically thick coma, the emitted photon does not escape directly but is resonantly scattered, leading to radiative excita-

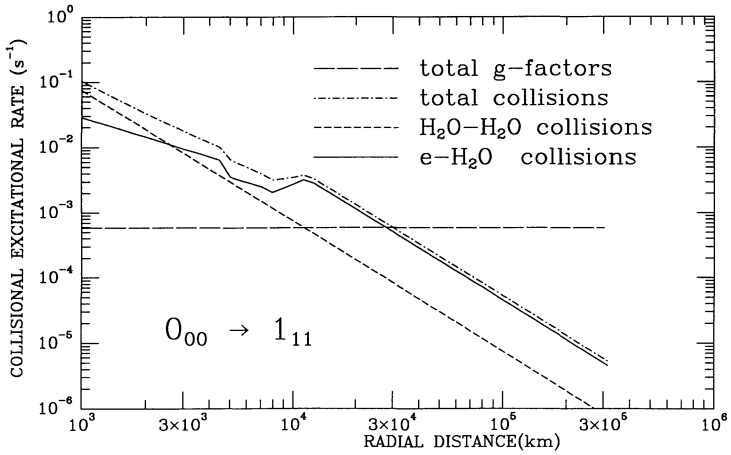

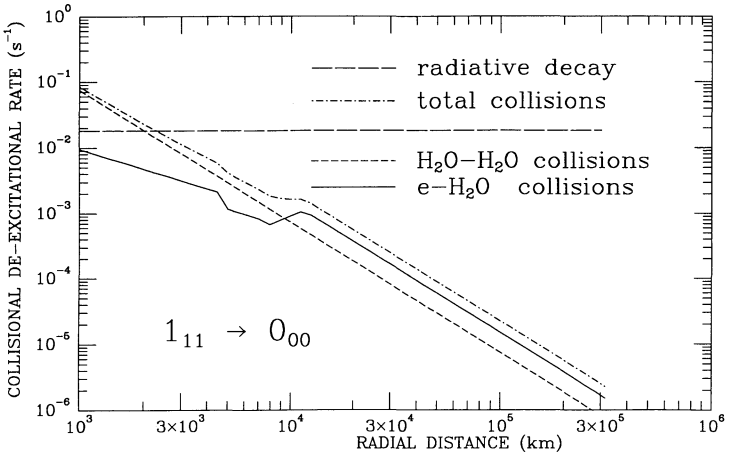

FIG. 3.—(*a*) The excitation rates for the $0_{00} \rightarrow 1_{11}$ rotational transition. The long-dash line represents the total g-factors (rates) for solar fluorescence including all vibrational bands at 0.9 AU. (*b*) The de-excitation rates for the $1_{11} \rightarrow 0_{00}$ rotational transitions. The long-dash line presents the Einstein coefficient for the transition, which corresponds to the radiative decay rate in the optically thin case.

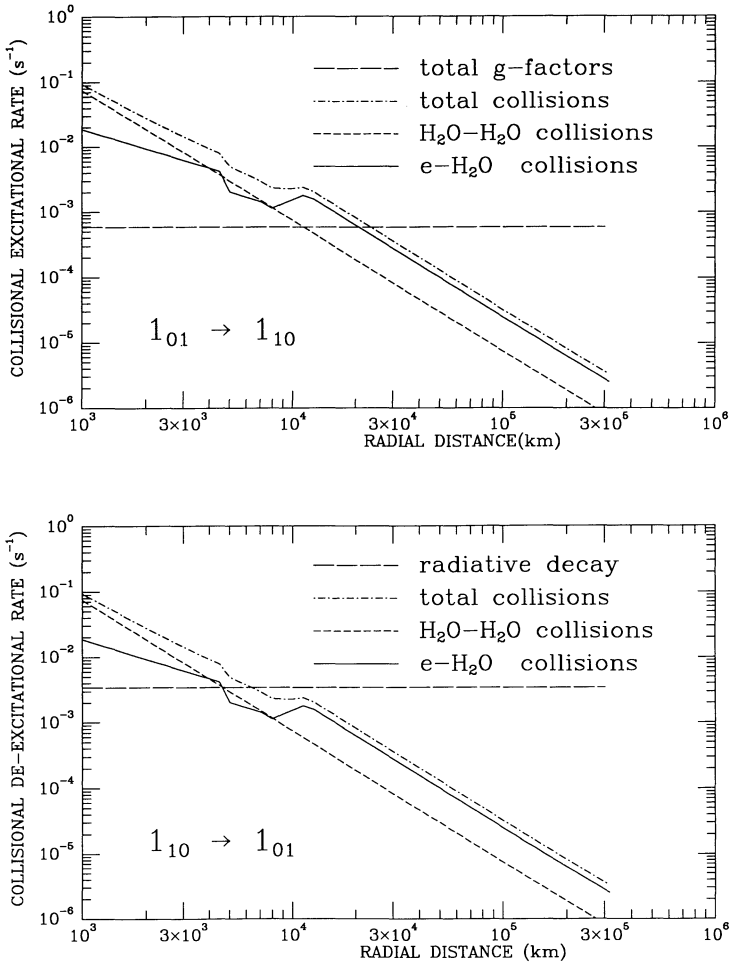

FIG. 4.—(*a*) The excitation rates for the $1_{01} \rightarrow 1_{10}$ rotational transition. The long-dash line represents the total *g*-factors (rates) for solar fluorescence including all vibrational bands at 0.9 AU. (*b*) The de-excitation rates for the $1_{10} \rightarrow 1_{01}$ rotational transitions. The long-dash line presents the Einstein coefficient for the transition, which corresponds to the radiative decay rate in the optically thin case.

tion of another water molecule to the upper excited level, reemission, and so on. Thus the average time spent in the excited level is increased by a factor of N_{esc}, and collisions have a correspondingly greater chance to relax the quantum in a rotational-translational process. Here N_{esc} is the average number of scatterings between the upper and lower energy levels before escaping the coma. To first order, rotational levels having radiative decay rates $(A) \leq N_{esc}\, \nu_{total}$ can be collisionally relaxed. The region sampled by the KAO observations is the intermediate coma ($r \leq \sim 1 \times 10^4$ km), where rotational lines of interest are optically thick; therefore, the effective radiative decay rates are reduced greatly (by ~80-fold, see Table 2 in the Appendix), owing to the effect of optical trapping.

5. DISCUSSION

As the result of optical trapping, we have a more extended inner coma, where collisional relaxation dominates and rotational excitation for cometary water is controlled by collisional effects, not by fluorescence. The temperature measured for the rotational states will be a measure of the electron or neutral kinetic temperatures, depending on cometocentric distance. In the intermediate region, where electron collisions dominate, the rotational temperature is undoubtedly controlled by electrons. We have followed Bockelee-Morvan (1987) in adopting a rotational cross section of 5×10^{-14} cm^2 for H_2O–H_2O collisions, which is the upper limit discussed in § 2.2. Therefore, the rates for neutral-neutral collisions have been (intentionally) greatly overestimated in our model, and electron-water collisions assume even greater significance. The effective rotational temperatures retrieved from KAO infrared spectra may reflect control of rotational populations by electrons, not by neutrals. The relationship between the observed rotational temperature and the neutral gas kinetic temperature may need to be reexamined in this case; however, a detailed treatment exceeds the scope of this paper.

The relative contribution of electron collisions depends on cometary activity. The size of the contact surface for the comet is determined by its gas production rate and generally increases with it. Therefore, for an active comet, we have a large collision-dominated inner region with relatively cool, and abundant, electrons which contribute significantly to rotational transitions and may dominate over neutral collisions in the intermediate region around the contact surface. In addition, most of the coma of interest to us is optically thick in the rotational lines, which enhances the significant role of colli-

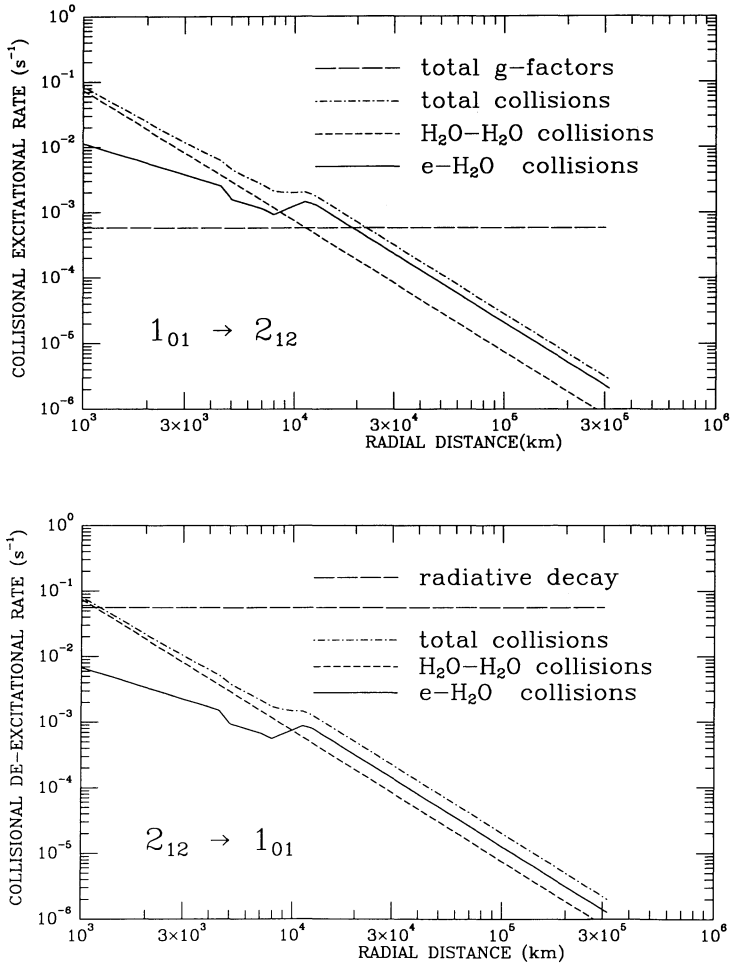

FIG. 5.—(*a*) The excitation rates for the $1_{01} \rightarrow 2_{12}$ rotational transition. The long-dash line represents the total *g*-factors (rates) for solar fluorescence including all vibrational bands at 0.9 AU. (*b*) The de-excitation rates for the $2_{12} \rightarrow 1_{01}$ rotational transitions. The long-dash line presents the Einstein coefficient for the transition, which corresponds to the radiative decay rate in the optically thin case.

sions in both exciting and de-exciting rotational transitions. For a less active comet, the collision-dominated inner region is much smaller, and the effect of optical trapping is important only in the very innermost coma. The excitation of rotational transitions is done mainly by solar fluorescence and the contribution of collisional excitation from both neutral-neutral and neutral-electron interactions is relatively small in this case.

In regard to ions, we know much about the ion environment in the comet but little about ion-water cross sections for rotational excitation at low impact energies (0.01–0.1 eV). Based on the expected D^2/E variation from the Born approximation, we expect that the ion-water cross section is at least 10^{-12} cm^2. Water-group ions such as H_3O^+ and H_2O^+ are the dominant ionic species in the coma, and their average relative velocity is $\sim 1/180$ of electrons. If ion–H_2O collisions are to equal e–H_2O collisions, their cross sections must be 180 times larger than those of electrons at the same impact energy, i.e., about 4×10^{-11} cm^2 at 0.02 eV. We hope to see theoretical calculations soon.

Although the above rough estimate of the relative contributions of e–H_2O and H_2O–H_2O collisions establishes the important role of electron collisions in comets, the question of whether electron collisions dominate the rotational population at a particular position in the intermediate coma is still somewhat model-dependent. A detailed assessment requires the exact forms of the electron temperature profile and of the electron density profile in the coma, and a better constraint on H_2O–H_2O collision cross sections from new experiments and model calculations. The most important parameter is electron temperature, and the determination of it requires a better understanding and detailed treatment of the heating and cooling processes of electrons in the magnetic-free and nonzero magnetic field region in the coma. Nevertheless, it is clear that electron collisions permit the rotational population to be controlled by collisional excitation in the intermediate coma, particularly in regions with optically thick rotational lines. The line-by-line intensities, seen in the KAO spectra and previously assigned to rotational equilibrium effected by neutral-neutral collisions in the intermediate coma, may instead be controlled by electron-neutral collisions.

6. SUMMARY

We have evaluated the significance of electron collisions with water molecules in the cometary coma. The present study combines electron excitation cross sections from theoretical calculations and laboratory measurements with parameters of

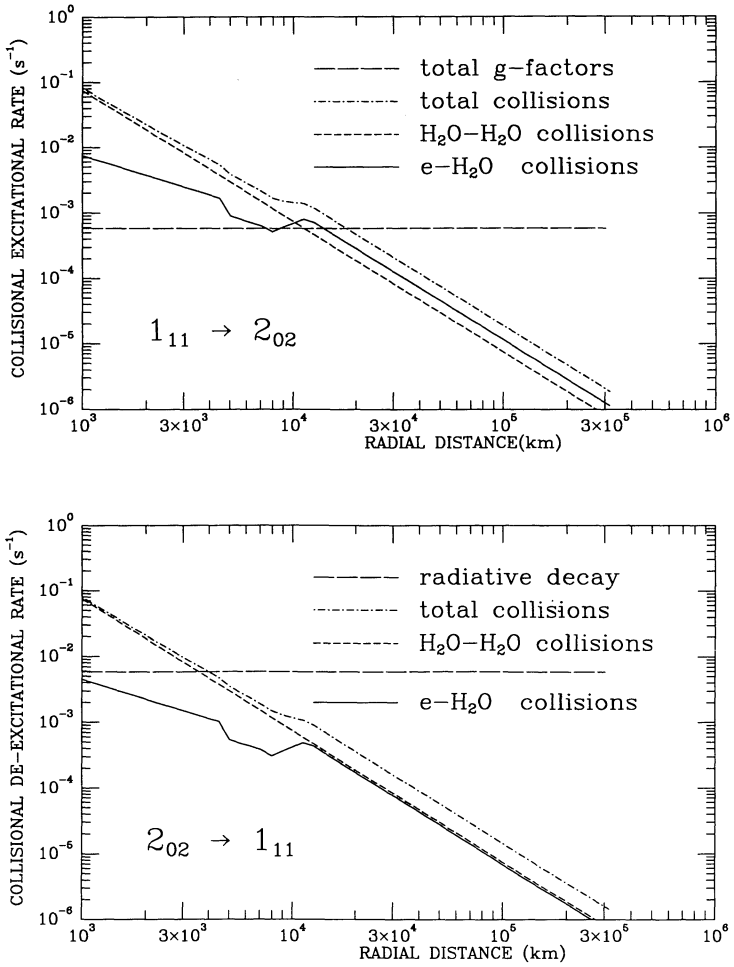

FIG. 6.—(*a*) The excitation rates for the $1_{11} \rightarrow 2_{02}$ rotational transition. The long-dash line represents the total *g*-factors (rates) for solar fluorescence including all vibrational bands at 0.9 AU. (*b*) The de-excitation rates for the $2_{02} \rightarrow 1_{11}$ rotational transitions. The long-dash line presents the Einstein coefficient for the transition, which corresponds to the radiative decay rate in the optically thin case.

the cometary plasma environment measured by *Giotto* and *Vega*. Electron collisional excitation is shown to be important in affecting rotational populations of the water molecule in the intermediate and outer coma of an active comet such as comet Halley. The effect of electron collisions is more prominent in the region in which the rotational lines are optically thick and may dominate neutral-neutral collisions over a significant part of the cometary coma.

We are indebted to R. Koch for his constructive comments on this paper. This research was supported by the Planetary Astronomy Program of the NASA Solar System Exploration Division under RTOP 196-41-54 to NASA/Goddard Space Flight Center.

APPENDIX

ESTIMATES OF N_{esc}

The estimates of the average number of scatterings can be done either with numerical integration or with Monte Carlo simulation by taking into account physical conditions and spectral line radiation transfer involved in the coma. For the simplified case of a homogeneous spherical atmosphere at rest with density varying as r^{-2}, the absorption coefficient at the radial distance r has the form

$$k(r) = k_0 \frac{r_0^2}{r^2}, \tag{A1}$$

TABLE 2

AVERAGE NUMBER OF SCATTERINGS N_{esc} FOR PHOTONS STARTING FROM RADIUS [$\tau = \tau(r, 0.0)$]

τ	Case 1 N_{esc}	Case 2 N_{esc}	τ	Case 1 N_{esc}	Case 2 N_{esc}
0.1.....	0.72	1.62	2.0	15.4	28.4
0.2.....	1.22	2.36	4.0	36.3	56.8
0.4.....	2.38	3.89	6.0	49.4	82.0
0.6.....	3.10	6.03	8.0	63.0	113
0.8.....	4.86	8.46	10.0	83.1	147
1.0.....	6.24	10.8	20.0	233	389

where k_0 is $k(r)$ at the radial distance r_0. At any radial distance r, the optical depth in the direction making an angle of θ with the radial direction is given as the following

$$\tau(r, \theta) = \frac{k_0 r_0^2}{r} \frac{\theta}{\sin(\theta)} . \tag{A2}$$

The average number of scatterings before escape for photons produced at radius r can be simulated by Monte Carlo method (Combi & Smyth 1988). The simulation is done as follows.

1. A photon is emitted isotropically outward (Case 1, $0.0 \leq \theta < 0.5\pi$) or isotropically (Case 2, $0.0 \leq \theta \leq \pi$) from the radius r_1 corresponding to optical depth $\tau(r_1, 0.0)$. The direction of the photon (θ, ϕ) is determined by

$$\theta = \arccos(1.0 - aR_i) \tag{A3}$$

$$\phi = 2\pi R_j , \tag{A4}$$

where θ and ϕ are polar angle and azimuthal angle with Z-axis in the radial direction. R_i and R_j are random numbers uniformly distributed from 0 to 1, and the parameter a is equal to 1.0 for Case 1 and 2.0 for Case 2. The distance S_1 traveled by the photon before being scattered at a point A is given by

$$\exp\left[- \int_0^{S_1} k(r) ds \right] = R_k , \tag{A5}$$

where R_k is a random number uniformly distributed from 0 to 1 and r is the radial distance of the point along the path.

2. The photon is absorbed at the point A, and reemitted isotropically in the new direction given by equation (A3) and equation (A4) ($a = 2.0$). It will then be scattered at a new position determined by equation (A5). The tracking of the photon continues until it escapes.

3. After running N photons the average number of scatterings before escape is obtained.

The result of such a simulation is given in Table 2. Although this rough treatment provides a useful guide to the reduction in effective radiative decay rates, it is of only limited value since the assumptions of spherical symmetry, homogeneity, and zero expansion velocity are not valid for real comets. A detailed model is needed for each rotational transition to determine N_{esc} as a function of optical depth, but we defer this analysis to a later paper. The principal effect of finite expansion velocity is a reduced optical depth owing to a difference in projected velocity for the emitter relative to the absorber.

REFERENCES

Balsiger, H., et al. 1986, Nature, 321, 330
Bauer, A., Godon, M., & Duterag, B. 1985, J. Quant. Spectrosc. Rad. Transf., 33, 167
Bockelee-Morvan, D. 1987, A&A, 181, 169
Bockelee-Morvan, D., & Crovisier, J. 1987a, A&A, 187, 425
———. 1987b, in Proc. Symposium On the Diversity and Similarity of Comets (ESA SP-278), p. 235
Chin, G., & Weaver, H. A. 1984, ApJ, 285, 858
Christophorou, L. G., & Pittman, D. 1970, J. Phys. B, 3, 1252
Combi, M. R. 1989, Icarus, 81, 41
Combi, M. R., & Smyth, W. H. 1988, ApJ, 327, 1026
Crovisier, J. 1984, A&A, 130, 361
Dickinson, A. S., & Richards, D. 1975, J. Phys. B, 8, 2846
Gan, L., & Cravens, T. E. 1990, J. Geophys. Res., 95, 6285
Hodges, R. R. 1990, Icarus, 83, 410
Ip, W. H., & Axford, W. I. 1990, in Physics and Chemistry of Comets, ed. F. Huebner (Berlin: Springer), 177
Ip, W. H., Schwenn, R., Rosenbauer, H., Balsiger, H., Neugebauer, M., & Shelly, E. G. 1987, A&A, 187, 132
Itikawa, Y. 1972, J. Phys. Soc. Japan, 32, 217
Jain, A., & Thompson, D. G. 1983, J. Phys. B, 16, 3077
Jung, K., Antoni, T., Müller, R., Kochem, K. H., & Ehrhardt, H. 1982, J. Phys. B, 15, 3535
King, G. W., Hainer, R. M., & Cross, P. C. 1947, Phys. Rev., 71, 443
Körösmezey, A., et al. 1987, J. Geophys. Res., 92, 7331
Krankowsky, D., et al. 1986, Nature, 321, 327
Lämmerzahl, P., et al. 1987, A&A, 187, 169
Larson, H. P., Weaver, H. A., Mumma, M. J., & Drapatz, S. 1989, ApJ, 338, 1106
Mumma, M. J., Weaver, H. A., Larson, H. P., Davis, D. S., & Williams, M. 1986, Science, 232, 1523
Murphy, J. S., & Boggs, J. E. 1969, J. Chem. Phys., 51, 3891
Neugebauer, M. 1990, Rev. Geophys., 28, 231
Pedersen, A., Grard, R., Trotignon, J. G., Beghin, C., Mikhailov, Y., & Mogilevsky, M. 1987, A&A, 187, 297
Schwendeman, R. H., & Laurie, V. W. 1958, Tables of Line Strengths for Rotational Transitions of Asymmetric Rotor Molecules (London: Pergamon)
Schwenn, R., Ip, W. H., Rosenbauer, H., Balsiger, H., Bühler, F., Goldstein, R., Meier, A., & Shelley, E. G. 1987, A&A, 187, 160
Sokolov, V. F., & Sokolova, Y. A. 1982, Sov. Tech. Phys. Lett., 7, 268
Storrs, A., & Mumma, M. J. 1991, private communication
Van Regemorter, H. 1965, ARA&A, 3, 71
Weaver, H. A., & Mumma, M. J. 1984, ApJ, 276, 782
Weaver, H. A., Mumma, M. J., & Larson, H. P. 1987, A&A, 187, 411